Original Article
Exosomes with IR780 and Lenvatinib loaded on GPC3 single-chain scFv antibodies for targeted hyperthermia and chemotherapy in hepatocellular carcinoma therapy

Shenan Huang[1*], Ming Xiong[1*], Jie Liu[2*], Jian Wang[3*], Xianyang Han[4*], Zhimeng Chen[5], Peiyi Xie[6], Zhipeng Zhou[7], Cong Liu[5], Hui Li[6], Zhili Wen[1], Xiaomei Huang[1], Binghai Zhou[5]

[1]Department of Gastroenterology, The Second Affiliated Hospital of Nanchang University, Nanchang 330006, Jiangxi, China; [2]Department of Hepatobiliary and Pancreatic Surgery, Zhongnan Hospital of Wuhan University, Wuhan 430071, Hubei, China; [3]Department of Hepato-Biliary-Pancreatic Surgery, Pingxiang People's Hospital, Pingxiang 337099, Jiangxi, China; [4]Department of Hepato-Biliary-Pancreatic Surgery, Wuyuan People's Hospital, Wuyuan, Shangrao 333200, Jiangxi, China; [5]Division of Hepato-Biliary-Pancreatic Surgery, Department of General Surgery, The Second Affiliated Hospital of Nanchang University, Nanchang 330006, Jiangxi, China; [6]Department of Liver Surgery and Transplantation, Liver Cancer Institute, Zhongshan Hospital, Fudan University, Shanghai 200032, China; [7]Department of General Surgery, Yifeng People's Hospital, Yifeng, Yichun 336300, Jiangxi, China. *Equal contributors.

Abstract: Exosomes (EXOs) are considered natural nanoparticles which have been widely used as carriers for the treatment and diagnosis of various diseases. However, due to the non-specific uptake, the unmodified EXOs cannot effectively deliver the vector to the target site. In this study, we used pDisplay vector to engineer Glypican-3 (GPC3) single-chain scFv antibody to the exosome surface, and the effect of engineered exosomes on the proliferation and migration of hepatocellular carcinoma (HCC) cells was determined by a series of in vitro experiments as well as in vivo mouse xenograft model and PDX model. Furthermore, we established an improved delivery system by engineering single-chain scFv antibody against GPC3 on the EXO surface for a more efficient HCC targeting. Moreover, the delivery system was loaded with IR780 and Lenvatinib for a combination of thermotherapy and chemotherapy. Our results revealed that the antibody-engineered exosomes enabled rapid imaging of HCC xenograft models post IR780 loading and showed significant anti-tumor photothermal therapy (PTT) effects after irradiation. Since dual loading of IR780 and Lenvatinib in exosomes required only a single injection and had a maximal efficacy against cancer cells, our findings highlight the clinical application of using GPC3 single-chain scFv antibody-engineered exosomes loaded with IR780 and Lenvartinib to achieve the imaging and the treatment of HCC from the combined effect of IR780-induced PTT and Lenvatinib-induced chemotherapy.

Keywords: GPC3 single chain antibody, exosomes, hepatocellular carcinoma, IR780, Lenvartinib

Introduction

Hepatocellular carcinoma (HCC) ranks the 5th most frequent cancer in men and the 9th in women as well as the second leading cause of tumor-related death worldwide [1, 2]. Currently, HCC treatment options mainly include surgical resection, targeted therapy, and immunotherapy [3]. Although recent advancement has increased the diagnosis rate and the treatment efficacy of HCC, the overall 5-year survival rate of HCC patients remains below 40% [4, 5]. Therefore, it is crucial to develop new and more effective treatment plans.

Glypican-3 (GPC3) is a 60-kDa cell surface protein of the phosphatidylinositol proteoglycan family. GPC3 has been reported to be highly expressed in various tumors, especially in HCC [6, 7]. In addition, the prognostic importance of serum GPC3 level and the immunoreactivity of GPC3 in tumor cells have been widely investigated in HCC patients [8, 9]. Besides as a biomarker, GPC3 is also considered as an important therapeutic target, and clinical trials targeting GPC3 are underway [10]. For example, Li et al. have developed GPC3-specific NK cells and explored their potential in the treatment of HCC [11].

Exosomes (EXOs) are lipid membrane nano-structures that are secreted by cells either directly from the plasma membrane or via the endocytic pathway [12, 13]. EXOs attract increasing attention in cancer therapy as EXOs have good biocompatibility, non-cytotoxicity, and low hemolysis, making them ideal carriers for delivering various drugs or biological materials in vitro and in vivo [14]. Nevertheless, the main challenge of the EXO-based delivery system is the localized delivery [15]. To overcome this limitation, exosomes have been conjugated with different target molecules to improve their expression in specific target tissues. For example, Mittal et al. and Cui et al. have reported different strategies of surface modification such as covalent modification and non-covalent modification as well as optical and radioactive isotope labelling of exosomes for imaging purpose [16, 17]. In other studies, EXOs are conjugated with target peptides or single-chain Fv (scFv) antibodies by covalent or bio-orthogonal reactions. Matin et al. attached high affinity anti-HER2 scFv antibody (ML39) on EXO surface to target breast cancer [18]. In this study, we engineered GPC3 single-chain scFv antibodies on EXOs for HCC tissue targeting as well as for the imaging and the delivery of photothermal therapy (PTT) and chemotherapy drug.

As one of the emerging cancer therapy, PTT uses the photothermal effect of photothermal agents to convert absorbed light energy into heat, resulting in thermal burns of tumors. PTT is a viable alternative to surgery for cancer treatment, exhibiting both noninvasive and tumor-specific effect [19] as it causes tumor necrosis and apoptosis by converting near-infrared (NIR) light to heat [20]. In addition to generating hyperthermia to ablate tumors, PTT also accelerates drug release from the delivery platform [21]. Therefore, integrating PTT inducers and chemotherapeutic agents into a single delivery system for a synergistic treatment is a promising strategy for treating various cancers, including HCC.

In phototherapy, the near infrared (NIR) light absorbers interact with NIR light (750-1000 nm) [22]; therefore, compared with traditional treatment, NIR phototherapy has higher selectivity for tumor area since only the light absorbers accumulated in the tumor area are activated by NIR light, thus reducing the side effects on healthy tissues. IR780 has an absorption peak at 780 nm, and it will generate temperature rise when interacting with NIR light. In addition, IR780 also emits high-intensity fluorescence in the wavelength range of 807-823 nm, making it useful for imaging applications [23, 24]. Thus, IR780 has been extensively studied as a promising target for cancer phototherapy and imaging. For example, Meng et al. have designed a nano-system based on tetrahedral DNA (Td) to deliver IR780 [25]. However, IR780 systemic delivery has been associated with poor water solubility and photostability, which affects its widespread use in imaging and PTT [26, 27]. In this study, we loaded IR780 in the GPC3 scFv antibody engineered EXOs to improve its targeting, stability, and functionality.

Lenvatinib, a small molecule inhibitor of receptor tyrosine kinases, has been approved as the first-line therapy for advanced unresectable HCC in many countries including in the United States, the European Union, Japan, and China [28-30]. It has an anti-tumor effect by inhibiting the activity of multiple receptor tyrosine kinases such the receptor for stem cell factor, platelet-derived growth factor receptor (PDGFR), fibroblast growth factor receptor (FGFR1-4), and vascular endothelial growth factor receptor (VEGFR1-3) [31, 32]. However, Lenvatinib produces many side effects such as vomiting, diarrhea hypertension, and proteinuria, and few studies have addressed this challenge by systematically delivering lower dose of lenvartinib to tumor sites to reduce the side effects and to maximize its anticancer activity.

In this study, EXOs derived from mesenchymal stem cells (MSCs) were initially engineered with GPC3 single-chain scFv antibodies and then loaded with IR780 and Lenvatinib (IL@GPC3-EXOs). We found that the GPC3 scFv engineered and IR780-loaded EXOs (IR780@GPC3-EXOs) could rapidly target HCC and trigger significant tumor suppression through photothermal effects after NIR. Dual loading of IR780 and Lenvartinib produced maximum antitumor effects after a single administration.

Materials and methods

Experimental reagents

MEM, DMEM, RPMI1640 medium were purchased from Hyclon, and fetal bovine serum

(FBS) was purchased from Gibco. Lenvartinib and IR780 were obtained from MedChemExpress (Shanghai, China) and RUIXI (Xian, China), respectively. An Annexin V-FITC/PI Apoptosis Detection Kit was obtained from Thermo Fisher Scientific and PKH67 kit was purchased from Sigma-Aldrich (St. Louis, USA).

Cell culture

HCC-LM3 cell lines were obtained from the Cell Bank of the Chinese Academy of Sciences (Shanghai, China). Cells were cultured in DMEM supplemented with 10% fetal bovine serum in a humidified 5% CO_2 incubator at 37°C.

Cell transfections

pDisplay vector plasmids were used for transfection. For cell transfection, one day in advance cells were seeded in six-well plates. Using Lipofectamine 3000 (Invitrogen), cells were transfected with the designated plasmids for 48 hours as directed by the manufacturer.

Exosomes isolation

Exosomes were isolated from genetically engineered mesenchymal stem cells using a Beckman ultracentrifuge. Briefly, the cells were centrifuged at 3,000 g for 15 min at 4°C, then at 20,000 g for 30 min at 4°C, followed by supernatant filtration with a 0.22 um membrane and centrifugated for 70 min at 100,000 g, 4°C. The EXOs was determined using a Zetasizer Nano ZS 90 particle size analyzer (Malvern Panalytical).

Encapsulation and drug loading efficiency

The encapsulation efficiency (EE) and drug loading (DL) were determined by high-performance liquid chromatography (HPLC) (UltiMate 3000). At a flow rate of 0.3 mL/min, samples were fed through the column to detect Lenvartinib at 210 nm. 200 μL of the sample was loaded onto a Slide-A-Lyzer MINI dialysis device (Thermo Fisher Scientific) and floated on PBS spun to obtain Lenvartinib release profile. At various times from the dialysis tube, as previously mentioned, each sample was examined by HPLC.

$$\text{Encapsulation efficiency} = \frac{\text{molecular weight loaded}}{\text{molecular weight initially added}} \times 100\%$$

Preparation and characterization of IL@GPC3-EXO

Briefly, GPC3-EXO (1×10^{10}/mL), IR780 (1 mg/mL), and Lenvartinib (1 mg/mL) were resuspended in 1 mL PBS. The mixture was electroporated at 400 volts for 1 ms. The cuvette liquid was then kept at 4°C for overnight incubation in an eppitube. The next day, to get rid of extra IR780 and Lenvartinib, the cuvette liquid was centrifuged for 90 minutes at 120,000 g. The IL@GPC3-EXO particles were resuspended in 1 mL PBS, their concentrations were detected by HPLC, and the EE and DL were calculated.

Xenograft model

Animal experiments were completed following institutional animal care and use committee (IACUC) approval. 6-week-old Balb/C nude male mice were obtained from Yawkang Co., Ltd. (Guangzhou, China). For tumorigenesis assay, we establish a xenograft tumor model by subcutaneous injection of HCC-LM3 tumor cells (1×10^6 in PBS). Two perpendicular diameters were measured to monitored tumor size every 3 days and nude mice were humanely sacrificed when the mice showed obvious discomfort or the average tumor volume [(length × width × width)/2] of the control group exceeded 2000 mm³, and all tumors were collected at the same time, and the subcutaneous tumors were removed, weighed, and their sizes were measured. The PTT regimen was given via tail vein injection. pbs; free IR780 (1 mg/kg) + NIR, IR780@EXO (1 mg/kg, 10^{10} EXO/mL) + NIR, and IR780@GPC3-EXO (1 mg IR780/kg, 10^{10} EXO/mL) + NIR. Post 24 hours of treatment, NIR irradiation was performed at the tumor site for 5 minutes.

Patient derived tumor xenograft (PDX) model

For the PDX model, tumor of PDX model was derived from HCC patients who have not receive any of the chemotherapy, radiotherapy, or targeted therapy. The tumor tissue sample was histologically confirmed as HCC samples by pathologists. Then, PDX tumor was rapidly cut into 3×3×3 mm³ pieces and then subcutaneously placed into the right forelimb of NCG (NCG (NOD/ShiLtJGpt-Prkdc[em26Cd52]Il2rg[em26Cd22]/Gpt)) male mice. When these tumors reached ~200 mm³, the mice were randomly divided

into four groups for antitumor studies and survival assessment. Once the tumor size reached 2000 mm³ or upon obvious signs of discomfort, mice were euthanized.

Cell proliferation assay and clone formation assay

Cell proliferation was examined by CCK-8 cell growth curve assay and clone formation assay. Assays were conducted as previously reported [33].

Migration and invasion assay

Scratch-wound healing assay and Transwell assay were performed based on a previously reported protocol [33].

Statistical analyses

Statistical analyses were performed using SPSS (version 25.0, Chicago, Illinois). T-test analysis performed using unpaired Students T-test. ANOVA approaches for longitudinal data include a repeated measure ANOVA and multivariate ANOVA (MANOVA). Kaplan-Meier method was performed for survival analysis. *P* values ≤ 0.05 were considered statistically significant differences.

Results

Production of GPC3 single-chain scFv antibody-engineered EXOs

The clinical application of artificially manufactured vectors as the delivery system is limited as they are assembled with organic or inorganic materials that are recognized by the innate immune system and are readily phagocytosed by macrophages and cleared by the reticuloendothelial system [15, 34]. On the other hand, EXOs have attracted greater interest in drug delivery due to their endogenous function and biocompatible composition from somatic cells [14]. In addition, recent studies have reported that MSCs-derived EXOs show a stable gene expression profile and have the potential for large-scale production [35, 36]. Therefore, we genetically engineered GPC3 single-chain scFv antibodies onto the surface of EXOs, so that these EXOs can target GPC3-positive tumors such as HCC.

To construct engineered EXOs, the GPC3 single-chain scFv antibody sequence [37] was inserted in the pDisplay vector which utilizes the transmembrane domain of PDGFR β and signaling peptide for transporting proteins across the plasma membrane [35, 38]. Subsequently, the single-chain scFv antibody-modified EXOs were obtained by density gradient centrifugation, followed by ultracentrifugation (**Figure 1A**). Western blotting (WB) confirmed the expression of the surface biomarkers of EXOs including CD63, CD81, CD9, and Alix, as well as the negative expression of Calnexin (**Figure 1B**). More importantly, the single chain scFv antibodies were detected by WB, indicating the successful integration of the antibody in the EXOs (**Figure 1B**). Nanoparticle Tracking Analysis (NTA) showed that the mean particle sizes of the Control-EXOs and GPC3-EXOs were 163 ± 28 and 189 ± 37, respectively (**Figure 1C**). Transmission electron microscope (TEM) revealed that the Control-EXOs and GPC3-EXOs comprised heterogeneous round/elliptical membranous vesicles of 60-180 nm, consistent with the data from NTA analysis (**Figure 1D**). Moreover, the corresponding zeta potentials of the Control-EXOs and GPC3-EXOs (ζ) were -21.6 ± 3.3 and -22.9 ± 4.8 mV, respectively (**Figure 1E**).

IR780 encapsulated in GPC3-EXO enabled rapid imaging in a mouse HCC model

To clarify whether GPC3-EXOs can recognize GPC3 antigen on the surface of the HCC cells, we carried out cellular ELISA and found that GPC3-EXOs indeed recognized native GPC3 antigen (**Figure 2A**). Furthermore, EXOs were labeled with PKH67 and co-cultured with HCC cells that had been fixed with paraformaldehyde. Immunofluorescence staining demonstrated that GPC3-EXOs was highly abundant in HCC cell membranes (**Figure 2B**), indicating that GPC3-EXOs could strongly recognize GPC3 protein on HCC cell membranes. Since EXOs must internalize to deliver agents into cancer cells, we performed immunofluorescence staining and found that GPC3-EXOs internalized into HCC cells effectively in a time-dependent manner. Specifically, during the initial 2 h incubation period, EXOs internalized; however, after 12 h of incubation, GPC3-EXOs internalization was significantly enhanced compared to Control-EXOs (**Figure 2C**), suggesting that the internalization of EXOs can be improved by the interaction between EXOs and the single-chain scFv antibody expressed on GPC3. Collectively, our
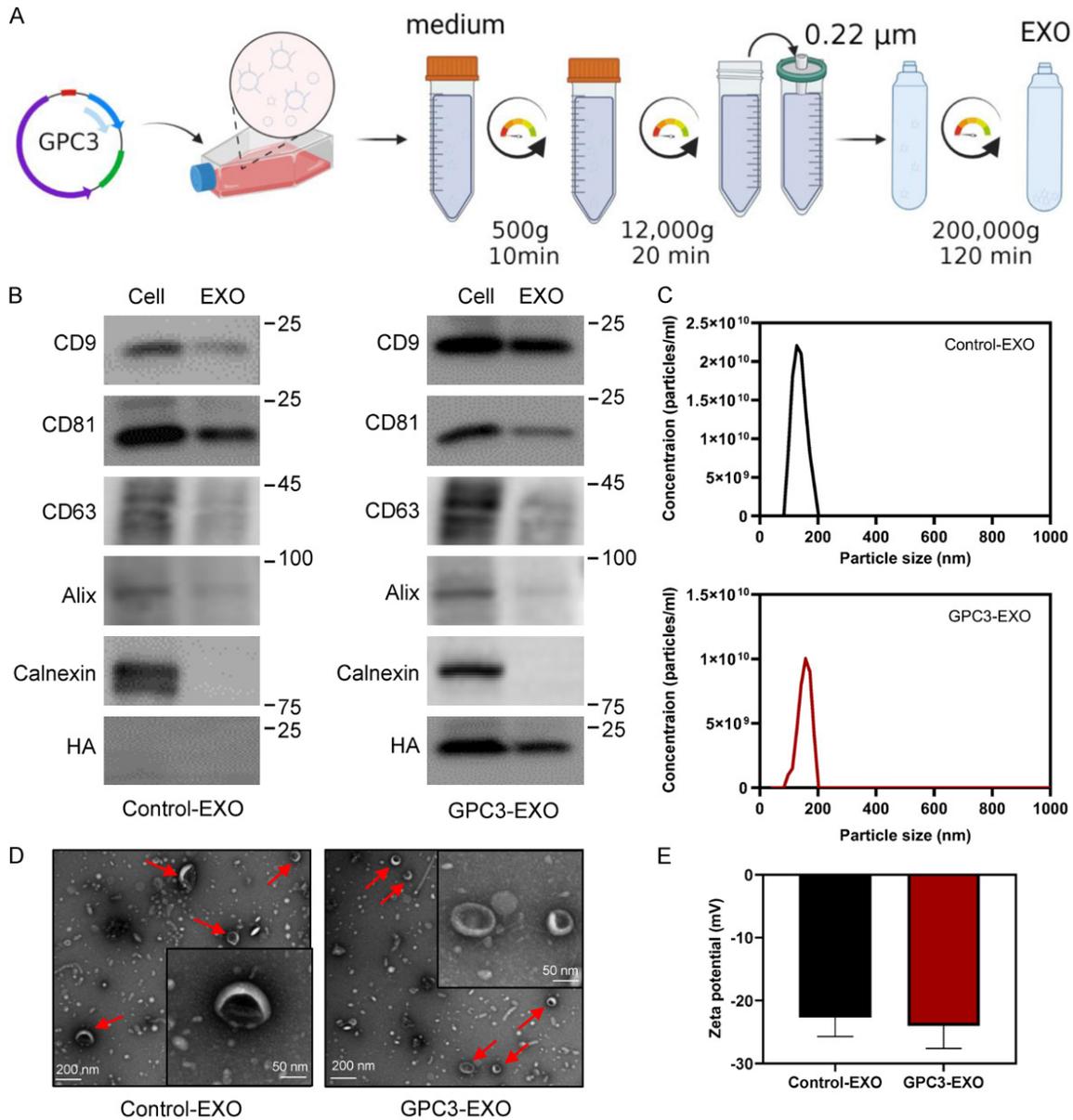
Figure 1. Design and identification of GPC3 engineered EXOs. A. Schematic diagram of the isolation of GPC3 engineered EXOs. B. Positive and negative biomarkers of EXOs. C. The particle size of EXOs measured by NTA. D. TEM images of EXOs. E. The zeta potential of EXOs was detected by NTA.

results indicate that engineering EXOs with GPC3 single chain scFv antibodies can improve the targeting ability of EXOs to HCC cells, thereby leading to an increased uptake of EXOs by HCC cells.

Furthermore, we investigated the ability of single-chain scFv body-engineered EXOs to encapsulate IR780 for HCC imaging in vivo. First, the loading rate of IR780 in EXOs was measured by HPLC (Figure S1), and its efficiency was ~80%

based on the plotted standard curve. Next, the tumor imaging capability of IR780@GPC3-EXOs was evaluated using a subcutaneous xenograft tumor model of HCC-LM3 cells. In vivo imaging system (IVIS) was used to detect IR780 biodistribution at predetermined time points. As a negative control, we confirmed that signal was not detected at any time in PBS treated mice. When compared with IR780 or IR780@EXOs, the signals produced by IR780@GPC3-EXOs on the tumor sites gradually increased from 4 hrs
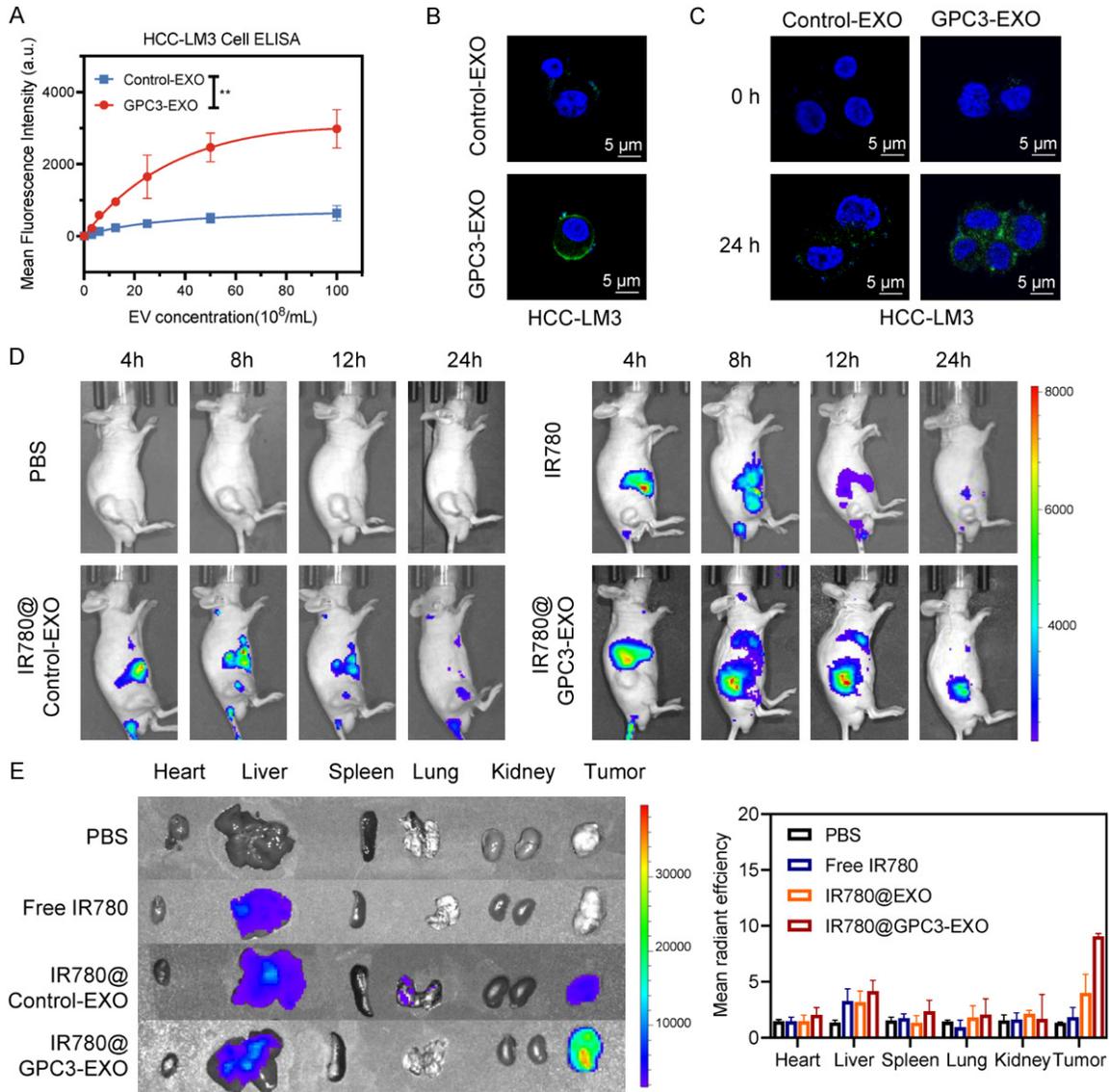
Figure 2. Cellular uptake and rapid imaging of GPC3-EXOs. A. Binding efficiency of GPC3-EXOs and Control-EXOs in HCC cells. B, C. Images of the PKH67-labeled GPC3-EXOs and Control-EXOs binding in HCC cells. Scale bars, 5 µm. D. Imaging and quantification of HCC-LM3-derived tumors after intravenous injection with PBS, free IR780, IR780@Control-EXOs, and IR780@GPC3-EXOs. IR780 dosage: 1 mg/kg. E. After in vivo imaging, Ex vivo imaging and quantification of dissected organs. **P < 0.01.

post-injection and peaked at 12 hrs post-injection. Importantly, at 24 hrs post-injection, the signals were mainly localized at the tumor site (**Figure 2D**). Consistently, in vitro fluorescence images of dissected tumors showed that compared to tumors treated with IR780 or IR780@EXOs, IR780@GPC3-EXO-treated tumors displayed the strongest signal (**Figure 2E**).

IR780@GPC3-EXOs suppressed HCC tumor progression through a photothermal effect

While the PTT-induced antitumor therapy offers several benefits, including being non-invasive,

controllable in space and time, with few adverse effects [20], the drawbacks of IR780 are poor water stability and the off-target effects of PTT. In contrast, our IR780@GPC3-EXOs approach could overcome these issues and achieved desirable effects. Using the treatment program as summarized in **Figure 3A**, the temperature in the PBS group did not significantly change after 5 minutes of NIR exposure, whereas the temperature of the IR780@GPC3-EXOs + NIR group dramatically increased (**Figure 3B**). In contrast to the free IR780 + NIR and IR780@EXOs + NIR groups, the IR780@GPC3-EXOs +
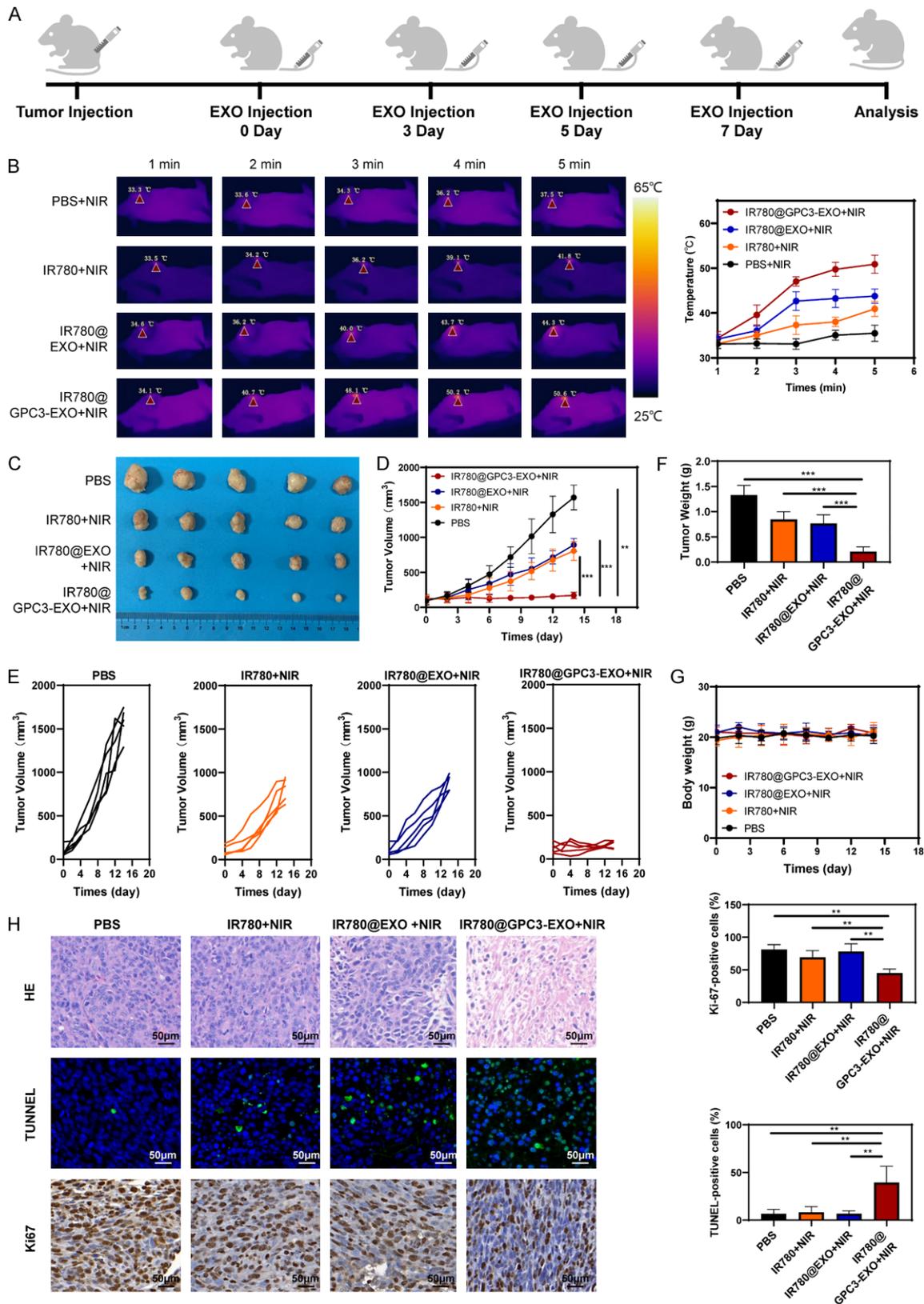
Figure 3. IR780@GPC3-EXO inhibits tumor growth. A. Schematic illustration of the treatment regimen. B. Thermal infrared photos of tumors and temperature monitoring during a 5-minute laser treatment. IR780: 1 mg/kg. C. Images of HCC-LM3-derived subcutaneous xenograft tumor. D, E. The tumor growth curve in different treatment groups. F.

The average weight of subcutaneous tumor mass in different groups. G. The mean body weight of mice in different groups. H. H&E, Ki-67, and TUNNEL staining of tumor samples from mice in the indicated treatment groups. Scale bars, 50 µm.

NIR group demonstrated the most pronounced tumor inhibition, although both groups strongly suppressed tumor growth (**Figure 3C-F**). Notably, no significant weight loss was observed in any treated groups (**Figure 3G**), and although H&E staining as well as viscera index data showed no obvious abnormality in major organs (Figure S2), more severe necrosis was observed in IR780@GPC3-EXOs + NIR group than in other groups (**Figure 3H**). Consistently, compared to other groups, IR780@GPC3-EXOs + NIR dramatically suppressed cell growth while promoted apoptosis, as determined by Ki-67 and Tunnel staining, respectively (**Figure 3H**).

IR780-mediated PTT promoted the release of Lenvartinib from GPC3-EXOs

Although PTT is a successful option in cancer treatment, the uneven distribution of heat within the tumor prevents its monotherapy from entirely destroying cancer cells [39]. Therefore, combinational therapy with PTT is the best strategy against cancer progression. Here, we explored the feasibility of GPC3-EXOs combined with IR780 and Lenvartinib, designated as IL@GPC3-EXOs, in inhibiting tumor growth. We first confirmed the encapsulation efficiencies of IR780 and Lenvartinib in EXOs to be 70% and 65%, respectively, by the standard curve (Figure S3). Since high colloidal stability is essential for the successful application of nanoparticle in vivo, we monitored IL@GPC3-EXOs suspension in PBS for 30 days and did not observe discernible change in particle size (**Figure 4A**). Then, drug release assays demonstrated that NIR light could stimulate the release of Lenvartinib from IL@GPC3-EXOs (**Figure 4B**), indicating that the dual loading of IR780 and Lenvartinib can successfully achieve the desired drug release under NIR laser control. Furthermore, we assessed the targeting capacity and therapeutic effectiveness of IL@GPC3-EXOs in vitro and found that IL@GPC4-EXOs + NIR had the strongest tumor-suppressing activity as determined by CCK-8 assay (**Figure 4C**), which was further confirmed by colony formation assay (**Figure 4D**). Moreover, wound healing assay and Transwell assay showed that IL@GPC3-EXOs + NIR significantly inhibited the migration and invasion of tumor cells (**Figure 4E**, **4F**). Taken together, these findings suggest that EXOs loaded with IR780 and Lenvartinib exert a more potent synergistic antitumor activity from IR780's photothermal and Lenvartinib's cytotoxic effects.

Single administration and irradiation of IL@GPC3-EXOs suppressed tumor growth in vivo

One of the major goals of combination therapy in cancer treatment is to lower the dose and frequency of delivery to reduce the side effect from treatment [40]; therefore, we determined whether combination therapy of IL@GPC3-EXOs and NIR could produce sustained tumor suppression in vivo. **Figure 5A** showed the schematic diagram of the experimental design. The temperature rising curve indicated that the temperature in IL@GPC3-EXOs + NIR treated tumors could reach to ~50°C (**Figure 5B**), and the combination therapy caused a stronger inhibition of tumor growth compared with heat or chemotherapy alone (**Figure 5C-F**). Notably, the body weight of all the treatment groups did not show significant alterations (**Figure 5G**), and the H&E staining of major organs indicated no overt anatomical abnormalities (Figure S4). Accordingly, the combined therapy dramatically increased the survival time of mice (**Figure 5H**). Interestingly, H&E staining revealed that the tumor cells in PBS-treated mice had distinct atypical nuclei, while the tumors from IL@GPC3-EXOs + NIR treated group had sparser and fibrous tissue (**Figure 5I**). In addition, Ki-67 staining and TUNNEL staining respectively revealed that tumor cells in IIL@GPC3-EXOs + NIR group had a smaller proportion of Ki-67-positive cells (**Figure 5I**), but more apoptotic cells than other groups did (**Figure 5I**).

A single administration of IL@GPC3-EXOs inhibited tumor growth and prolonged survival in the HCC PDX model

PDX model has been widely used as the in vivo model for drug evaluation [41, 42]. Therefore, we created a HCC PDX model to evaluate if GPC3-EXOs could serve as a delivery system with clinical and translational value that pro-
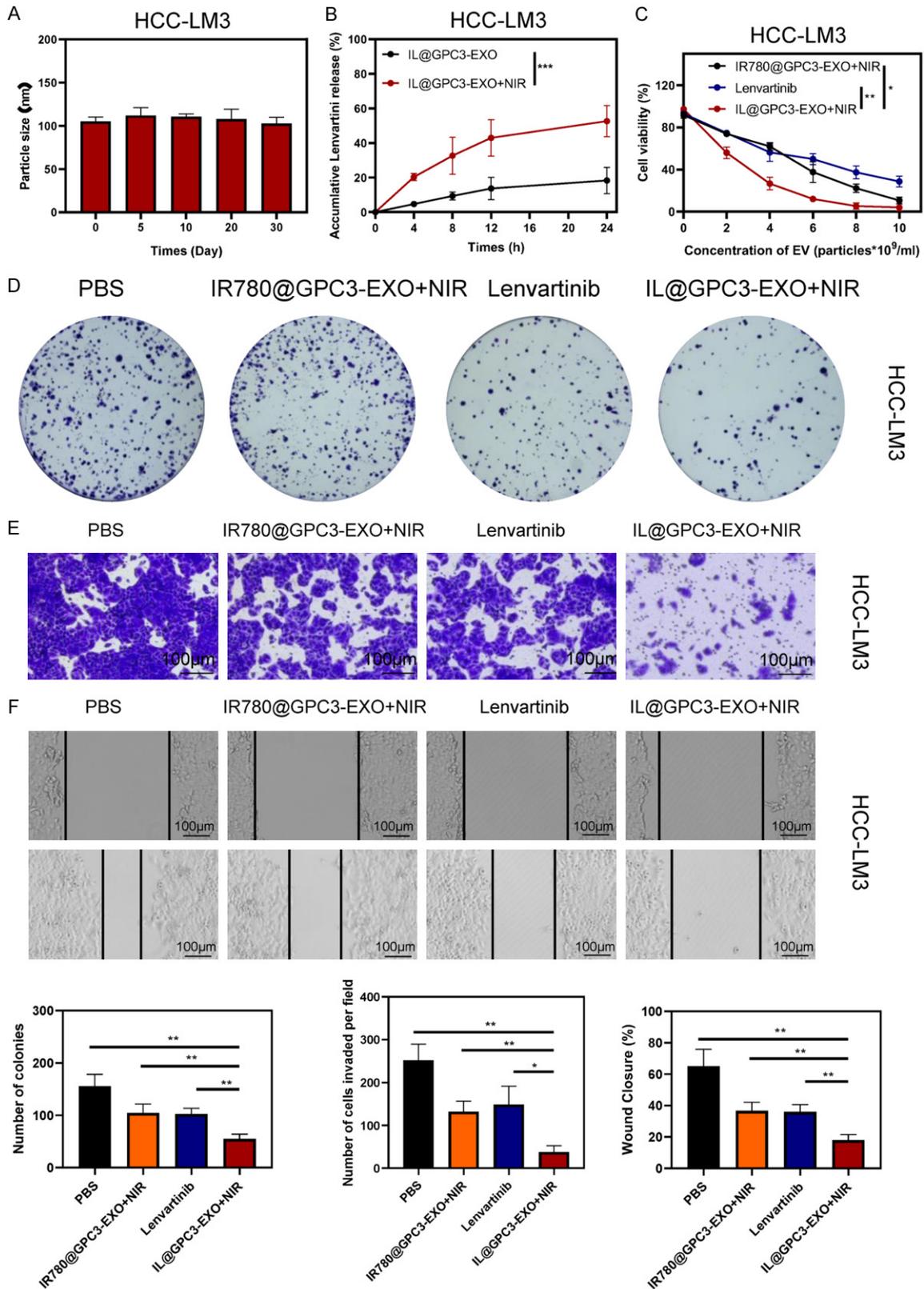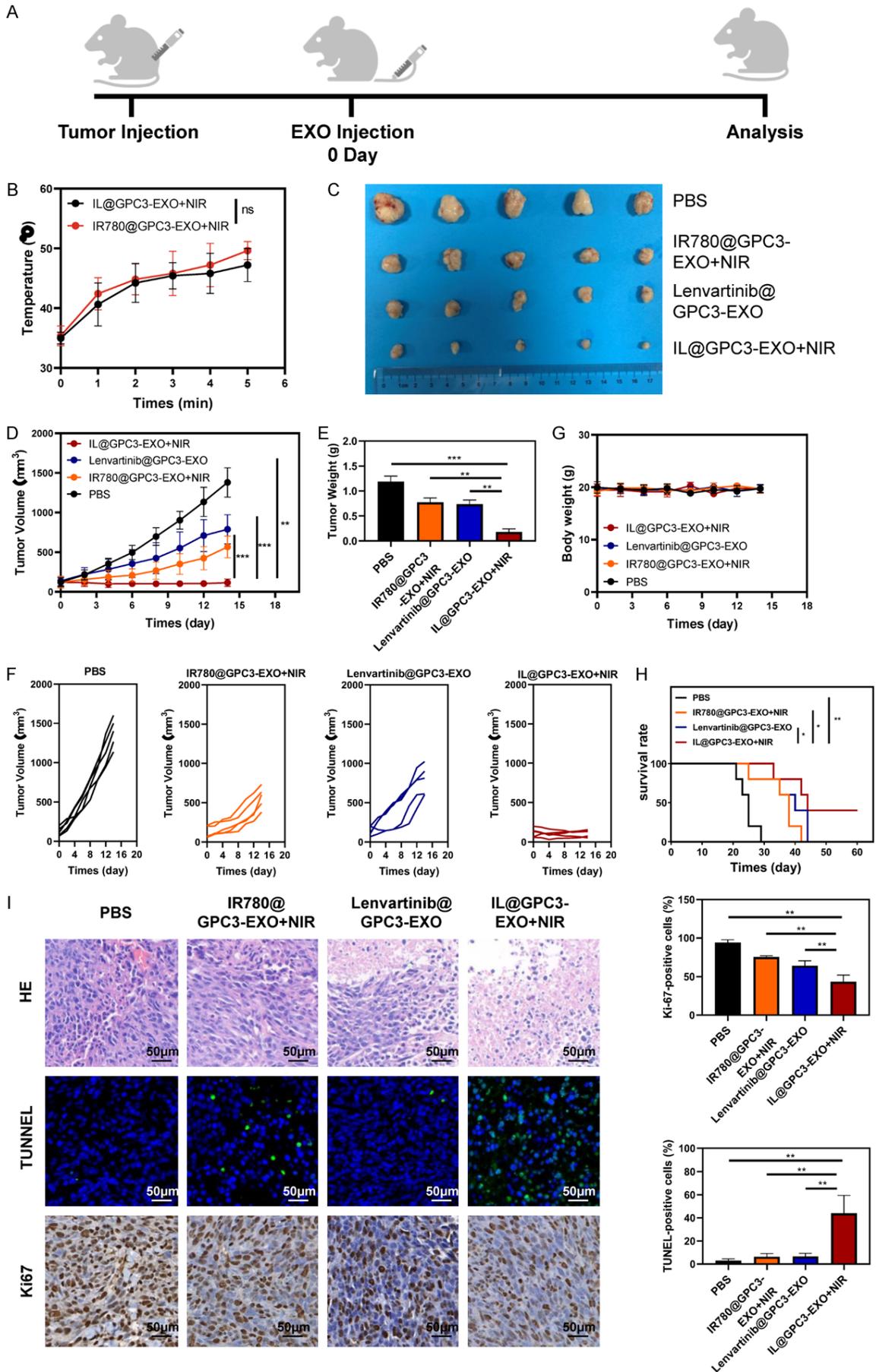
Figure 4. Combination of IL@GPC3-EXOs + NIR enhances the release of Lenvartinib and exerts a synergistic inhibitory effect on HCC growth in vitro. A. The particle size of EXOs detected by NTA within 30 days. B. Lenvartinib release profiles from IL@GPC3-EXOs with/without NIR irradiation. C. The viability of cells after indicated treatments. D. Colony formation assay of HCC cells after various treatments. E, F. The migration and invasion of cells after various treatments. Scale bars, 100 μm.

Figure 5. Combination of IL@GPC3-EXOs + NIR causes sustained tumor suppression effects. A. The flowchart of study design. B. Temperature in tumors during 24 h laser irradiation. C. The appearance of the tumor at the end of the treatment. D. Tumor growth curves after various treatments. E. Tumor weight in mice of different groups. F. Individual tumor growth curve. G. Mean body weight of mice in different groups. H. The survival rates of mice in different groups. I. H&E, Ki-67, and TUNNEL staining of tumors from various groups. Scale bars, 50 µm.
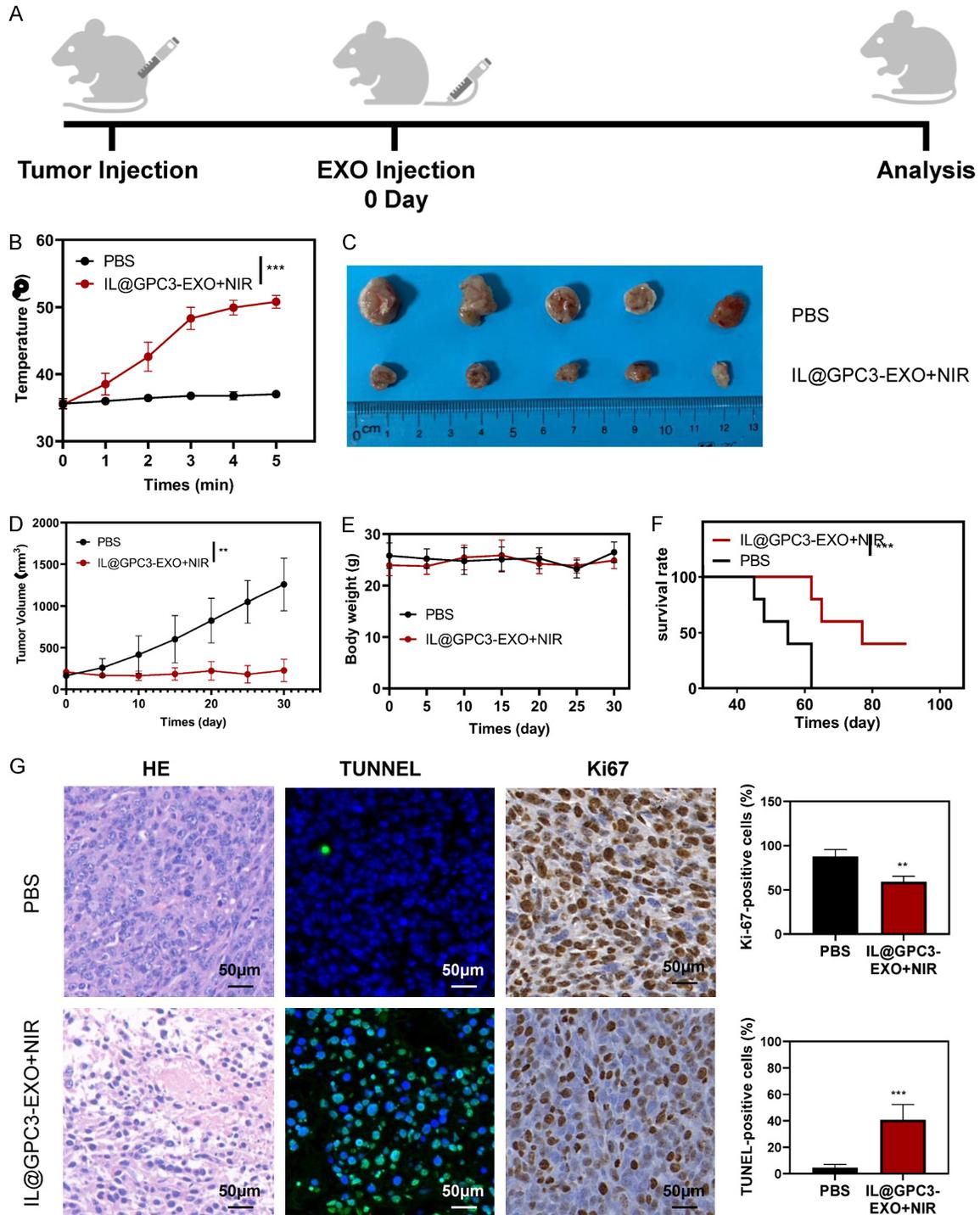
Figure 6. Significant anti-tumor effects of IL@GPC3-EXOs in HCC PDX model. A. Schematic diagram of treatment strategy. B. Temperature in tumors under laser treatment following intravenous injections. C, D. Tumor growth curves after indicated treatment. E. Body weight of mice treated with various agents. F. Overall survival of mice with the various treatment. G. TUNNEL, Ki-67, and H&E staining of tumors from various groups. Scale bars, 50 µm.

vides drugs and photothermal materials for HCC treatment. The schematic diagram of the experimental design is shown in **Figure 6A**. The infra-red thermal imaging revealed that the temperature in IL@GPC3-EXOs + NIR treated tumors increased to approximately 50°C, which was similar to the rising temperature of the tumor in the above cell line derived xenograft (CDX) model (**Figure 6B**). In line with this finding, IL@GPC3-EXOs + NIR significantly suppressed tumor growth compared to the PBS group (**Figure 6C**, **6D**). The body weight of NCG mice in all groups remained unchanged during treatment (**Figure 6E**). Consistently, IL@GPC3-EXOs + NIR increased the survival of mice (**Figure 6F**) and a smaller proportion of Ki-67-positive cells (**Figure 6G**), but more apoptotic cells than PBS group (**Figure 6G**), and H&E staining of the major organs showed no overt anatomical abnormalities (Figure S5). To further assess the possible systemic toxicity, routine blood tests and blood biochemistry tests were performed, and the results indicated that the functional parameters were within the normal range after treatment (Figure S6A, S6B). All these data suggest that IL@GPC3-EXOs could serve as a promising and effective therapeutic modality for HCC. GPC3 single-chain scFv antibody-engineered EXOs can be employed as a unique nano-delivery platform for targeted therapy of GPC3-positive HCC patients.

Discussion

The therapeutic effect of HCC is limited by several factors: the nonspecific killing of drugs, inflammatory reaction, and immune rejection. In this study, GPC3 single chain scFv antibodies engineered on the surface of EXOs showed increased targeting to HCC in vitro and in vivo. These engineered EXOs can not only produce fluorescence imaging in tumors within 24 hrs after loading the imaging probe IR780 but also serve as a novel nano-delivery platform for photothermal therapy. In addition, they can deliver therapeutic agents such as IR780 or Lenvartinib alone or together to achieve synergistic therapeutic effects through a single administration.

Lenvartinib is generally used to treat patients with unresectable HCC. At present, no effective strategy has been developed to implement the controlled release of Lenvartinib. The lipid bilayer structure of EXOs makes them an ideal carrier for delivering therapeutic drugs or biomaterials, which can further protect the activity of Lenvartinib. Therefore, in this study, we loaded Lenvartinib into the engineering EXOs and assessed their tumor-suppressing activity in CDX and PDX models. Our data suggest that GPC3-EXOs are a reliable and effective nano-delivery system with excellent clinical and translational potential.

The current study does, however, have several limitations. First, despite GPC3-EXOs can effectively bind to human GPC3 protein, additional research is required for their therapeutic application. For instance, the difference in the expression level of GPC3 in HCC is the most critical determinant affecting the delivery efficiency of GPC3-EXOs. Secondly, it is still challenging in exosomes extraction and storage, which needs standardized guidelines. Finally, the development of carriers with higher tumor targeting efficiency is the focus of future research, which will greatly improve the current drug delivery situation. Although EXOs-based delivery system presents some obstacles and difficulties, this single-chain scFv antibody-modified EXO strategy has great potential in the field of cancer therapy.

Acknowledgements

Disclosure of conflict of interest

None.

Address correspondence to: Binghai Zhou, Division of Hepato-Biliary-Pancreatic Surgery, Department of General Surgery, The Second Affiliated Hospital of Nanchang University, No. 1, Minde Road, Nanchang 330006, Jiangxi, China. E-mail: 18888291342@163.com; Xiaomei Huang, Department of Gastroenterology, The Second Affiliated Hospital of Nanchang University, Nanchang 330006, Jiangxi, China. E-mail: h365112954@163.com

References

[1] Hepatocellular carcinoma. Nat Rev Dis Primers 2021; 7: 7.

[2] Bruix J and Sherman M; Practice Guidelines Committee, American Association for the Study of Liver Diseases. Management of hepatocellular carcinoma. Hepatology 2005; 42: 1208-1236.

[3] Hartke J, Johnson M and Ghabril M. The diagnosis and treatment of hepatocellular carcinoma. Semin Diagn Pathol 2017; 34: 153-159.

[4] Parikh ND and Pillai A. Recent advances in hepatocellular carcinoma treatment. Clin Gastroenterol Hepatol 2021; 19: 2020-2024.

[5] Wallace MC, Preen D, Jeffrey GP and Adams LA. The evolving epidemiology of hepatocellular carcinoma: a global perspective. Expert Rev Gastroenterol Hepatol 2015; 9: 765-779.

[6] Du K, Li Y, Liu J, Chen W, Wei Z, Luo Y, Liu H, Qi Y, Wang F and Sui J. A bispecific antibody targeting GPC3 and CD47 induced enhanced antitumor efficacy against dual antigen-expressing HCC. Mol Ther 2021; 29: 1572-1584.

[7] Nishida T and Kataoka H. Glypican 3-Targeted therapy in hepatocellular carcinoma. Cancers (Basel) 2019; 11: 1339.

[8] Shimizu Y, Suzuki T, Yoshikawa T, Endo I and Nakatsura T. Next-generation cancer immunotherapy targeting glypican-3. Front Oncol 2019; 9: 248.

[9] Fu Y, Urban DJ, Nani RR, Zhang YF, Li N, Fu H, Shah H, Gorka AP, Guha R, Chen L, Hall MD, Schnermann MJ and Ho M. Glypican-3-specific antibody drug conjugates targeting hepatocellular carcinoma. Hepatology 2019; 70: 563-576.

[10] Zhou F, Shang W, Yu X and Tian J. Glypican-3: a promising biomarker for hepatocellular carcinoma diagnosis and treatment. Med Res Rev 2018; 38: 741-767.

[11] Yu M, Luo H, Fan M, Wu X, Shi B, Di S, Liu Y, Pan Z, Jiang H and Li Z. Development of GPC3-specific chimeric antigen receptor-engineered natural killer cells for the treatment of hepatocellular carcinoma. Mol Ther 2018; 26: 366-378.

[12] Pegtel DM and Gould SJ. Exosomes. Annu Rev Biochem 2019; 88: 487-514.

[13] Song J, Liu Y, Chen Q, Yang J, Jiang Z, Zhang H, Liu Z and Jin B. Expression patterns and the prognostic value of the SMYD family members in human breast carcinoma using integrative bioinformatics analysis. Oncol Lett 2019; 17: 3851-3861.

[14] Batrakova EV and Kim MS. Using exosomes, naturally-equipped nanocarriers, for drug delivery. J Control Release 2015; 219: 396-405.

[15] Kalluri R and LeBleu VS. The biology, function, and biomedical applications of exosomes. Science 2020; 367: eaau6977.

[16] Zhou Y, Zhang Y, Gong H, Luo S and Cui Y. The role of exosomes and their applications in cancer. Int J Mol Sci 2021; 22: 12204.

[17] Salunkhe S, Dheeraj, Basak M, Chitkara D and Mittal A. Surface functionalization of exosomes for target-specific delivery and in vivo imaging & tracking: strategies and significance. J Control Release 2020; 326: 599-614.

[18] Wang JH, Forterre AV, Zhao J, Frimannsson DO, Delcayre A, Antes TJ, Efron B, Jeffrey SS, Pegram MD and Matin AC. Anti-HER2 scFv-directed extracellular vesicle-mediated mRNA-based gene delivery inhibits growth of HER2-positive human breast tumor xenografts by prodrug activation. Mol Cancer Ther 2018; 17: 1133-1142.

[19] Liu Y, Bhattarai P, Dai Z and Chen X. Photothermal therapy and photoacoustic imaging via nanotheranostics in fighting cancer. Chem Soc Rev 2019; 48: 2053-2108.

[20] Shi H and Sadler PJ. How promising is phototherapy for cancer? Br J Cancer 2020; 123: 871-873.

[21] Zhen X, Cheng P and Pu K. Recent advances in cell membrane-camouflaged nanoparticles for cancer phototherapy. Small 2019; 15: e1804105.

[22] Alves CG, Lima-Sousa R, de Melo-Diogo D, Louro RO and Correia IJ. IR780 based nanomaterials for cancer imaging and photothermal, photodynamic and combinatorial therapies. Int J Pharm 2018; 542: 164-175.

[23] Gao D, Shi Y, Ni J, Chen S, Wang Y, Zhao B, Song M, Guo X, Ren X, Zhang X, Tian Z and Yang Z. NIR/MRI-guided oxygen-independent carrier-free anti-tumor nano-theranostics. Small 2022; 18: e2106000.

[24] Potara M, Nagy-Simon T, Focsan M, Licarete E, Soritau O, Vulpoi A and Astilean S. Folate-targeted Pluronic-chitosan nanocapsules loaded with IR780 for near-infrared fluorescence imaging and photothermal-photodynamic therapy of ovarian cancer. Colloids Surf B Biointerfaces 2021; 203: 111755.

[25] Wang S, Liu Z, Tong Y, Zhai Y, Zhao X, Yue X, Qiao Y, Liu Y, Yin Y, Xi R, Zhao W and Meng M. Improved cancer phototheranostic efficacy of hydrophobic IR780 via parenteral route by association with tetrahedral nanostructured DNA. J Control Release 2021; 330: 483-492.

[26] Zhang T, Wu B, Akakuru OU, Yao C, Sun S, Chen L, Ren W, Wu A and Huang P. Hsp90 inhibitor-loaded IR780 micelles for mitochondria-targeted mild-temperature photothermal therapy in xenograft models of human breast cancer. Cancer Lett 2021; 500: 41-50.

[27] Zhang TX, Hou X, Kong Y, Yang F, Yue YX, Shah MR, Li HB, Huang F, Liu J and Guo DS. A hypoxia-responsive supramolecular formulation for imaging-guided photothermal therapy. Theranostics 2022; 12: 396-409.

[28] Al-Salama ZT, Syed YY and Scott LJ. Lenvatinib: a review in hepatocellular carcinoma. Drugs 2019; 79: 665-674.

[29] Shi T, Iwama H, Fujita K, Kobara H, Nishiyama N, Fujihara S, Goda Y, Yoneyama H, Morishita A, Tani J, Yamada M, Nakahara M, Takuma K and Masaki T. Evaluating the effect of lenvatinib on sorafenib-resistant hepatocellular carcinoma cells. Int J Mol Sci 2021; 22: 13071.

[30] Zhao Y, Zhang YN, Wang KT and Chen L. Lenvatinib for hepatocellular carcinoma: from preclinical mechanisms to anti-cancer therapy. Biochim Biophys Acta Rev Cancer 2020; 1874: 188391.

[31] Llovet JM, Montal R, Sia D and Finn RS. Molecular therapies and precision medicine for hepatocellular carcinoma. Nat Rev Clin Oncol 2018; 15: 599-616.

[32] Zheng Y, Huang C, Lu L, Yu K, Zhao J, Chen M, Liu L, Sun Q, Lin Z, Zheng J, Chen J and Zhang J. STOML2 potentiates metastasis of hepatocellular carcinoma by promoting PINK1-mediated mitophagy and regulates sensitivity to lenvatinib. J Hematol Oncol 2021; 14: 16.

[33] Xia P, Zhang H, Xu K, Jiang X, Gao M, Wang G, Liu Y, Yao Y, Chen X, Ma W, Zhang Z and Yuan Y. MYC-targeted WDR4 promotes proliferation, metastasis, and sorafenib resistance by inducing CCNB1 translation in hepatocellular carcinoma. Cell Death Dis 2021; 12: 691.

[34] Xia P, Yuan H, Tian M, Zhong T, Hou R, Xu X, Ma J, Wang H, Li Z, Huang D, Qu C, Dai L, Xu C, Yang C, Jiang H, He Y, Rückert F, Li Z, Yuan Y and Wang J. Surface-engineered extracellular vesicles with CDH17 nanobodies to efficiently deliver imaging probes and chemo-photothermal drugs for gastric cancer theragnostic. Advanced Functional Materials 2023; 33: 2209393.

[35] Harrell CR, Jovicic N, Djonov V, Arsenijevic N and Volarevic V. Mesenchymal stem cell-derived exosomes and other extracellular vesicles as new remedies in the therapy of inflammatory diseases. Cells 2019; 8: 1605.

[36] Lai RC, Yeo RW and Lim SK. Mesenchymal stem cell exosomes. Semin Cell Dev Biol 2015; 40: 82-88.

[37] Li Y, Siegel DL, Scholler N and Kaplan DE. Validation of glypican-3-specific scFv isolated from paired display/secretory yeast display library. BMC Biotechnol 2012; 12: 23.

[38] Liu ZY, Wang W, Jin B, Li GZ, Du G, Zhang ZL, Han LT, Huang GZ and Tang ZY. Protection against ischemia-reperfusion injury in aged liver donor by the induction of exogenous human telomerase reverse transcriptase gene. Transplant Proc 2014; 46: 1567-1572.

[39] Ma D, Du G, Yang J, Song J, Ma H, Wang J, Zhang T and Jin B. Clinical application of a modified double purse-string continuous suture technique for pancreaticojejunostomy: reliable for laparoscopic surgery and small size main pancreatic duct. Biomed Res Int 2021; 2021: 6676999.

[40] Tian R, Wang Z, Niu R, Wang H, Guan W and Chang J. Tumor exosome mimicking nanoparticles for tumor combinatorial chemo-photothermal therapy. Front Bioeng Biotechnol 2020; 8: 1010.

[41] Hidalgo M, Amant F, Biankin AV, Budinska E, Byrne AT, Caldas C, Clarke RB, de Jong S, Jonkers J, Maelandsmo GM, Roman-Roman S, Seoane J, Trusolino L and Villanueva A. Patient-derived xenograft models: an emerging platform for translational cancer research. Cancer Discov 2014; 4: 998-1013.

[42] Yoshida GJ. Applications of patient-derived tumor xenograft models and tumor organoids. J Hematol Oncol 2020; 13: 4.
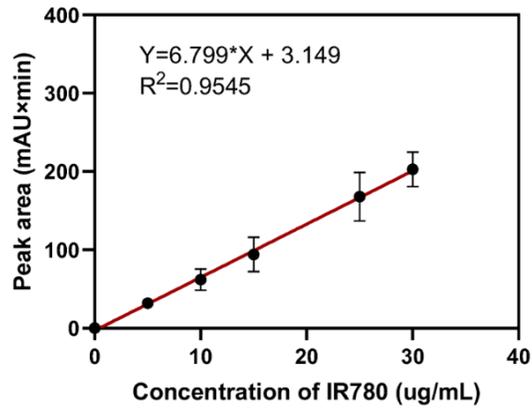
Figure S1. IR780 standard curves based on absorbance/concentration and HPLC peak area/concentration constructed using a serially diluted standard template (*n*=3).
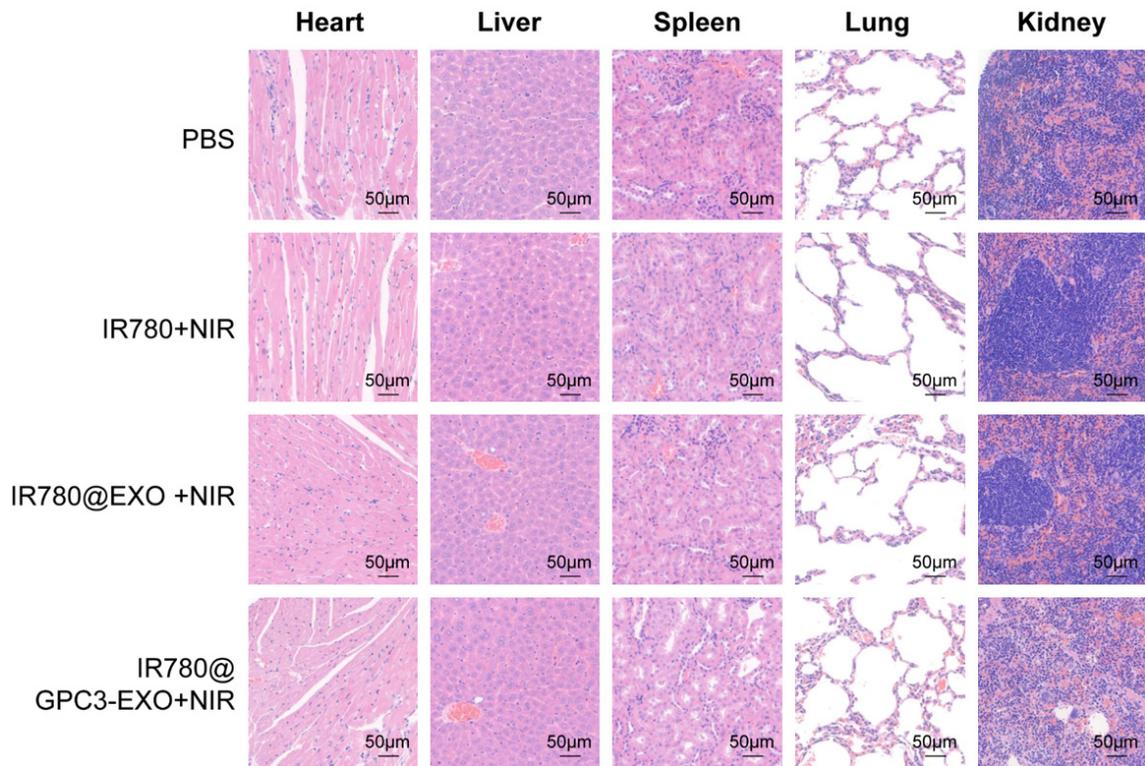

Figure S2. H&E staining for major organs (heart, liver, spleen, lung, kidney) in each group. Scale bars, 50 μm.
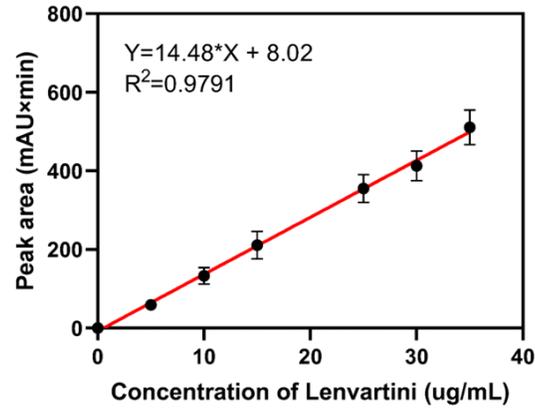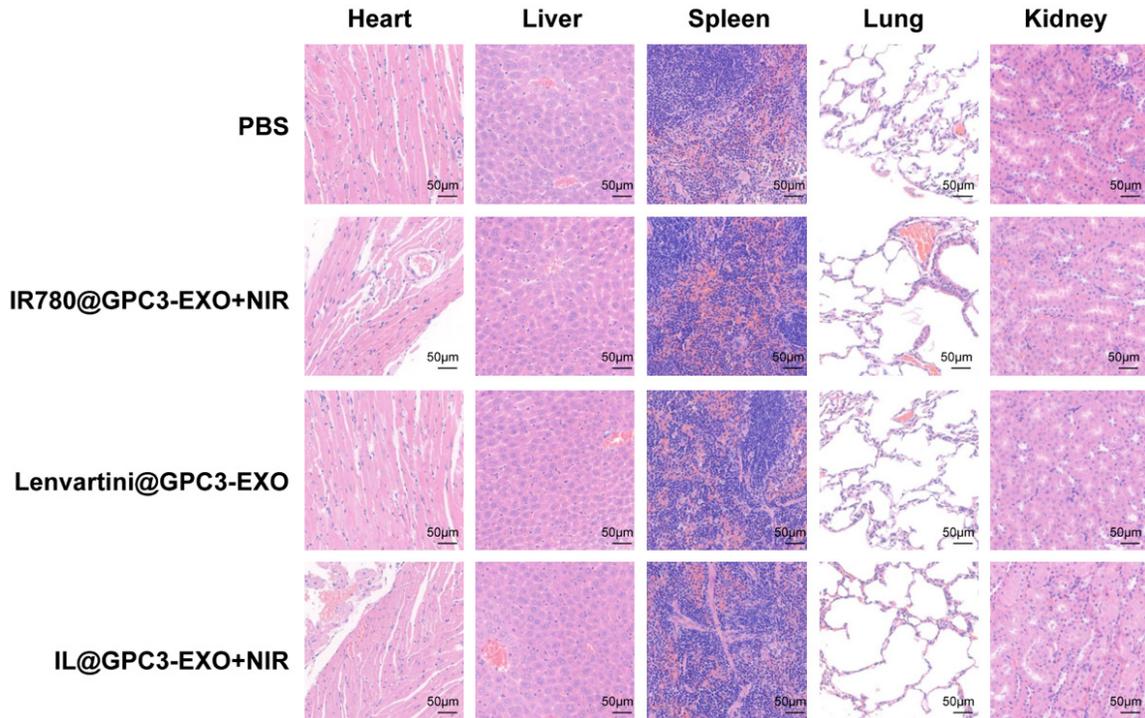
Figure S3. Lenvartini standard curves based on absorbance/concentration and HPLC peak area/concentration constructed using a serially diluted standard template (n=3).

Figure S4. H&E staining for major organs (heart, liver, spleen, lung, kidney) from mice. Scale bars, 50 μm.
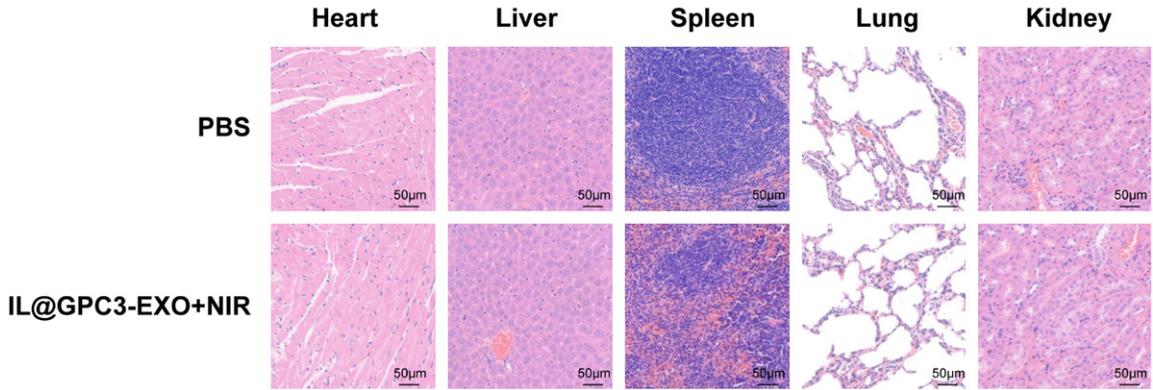
Figure S5. H&E staining for major organs (heart, liver, spleen, lung, kidney) from mice. Scale bars, 50 μm.
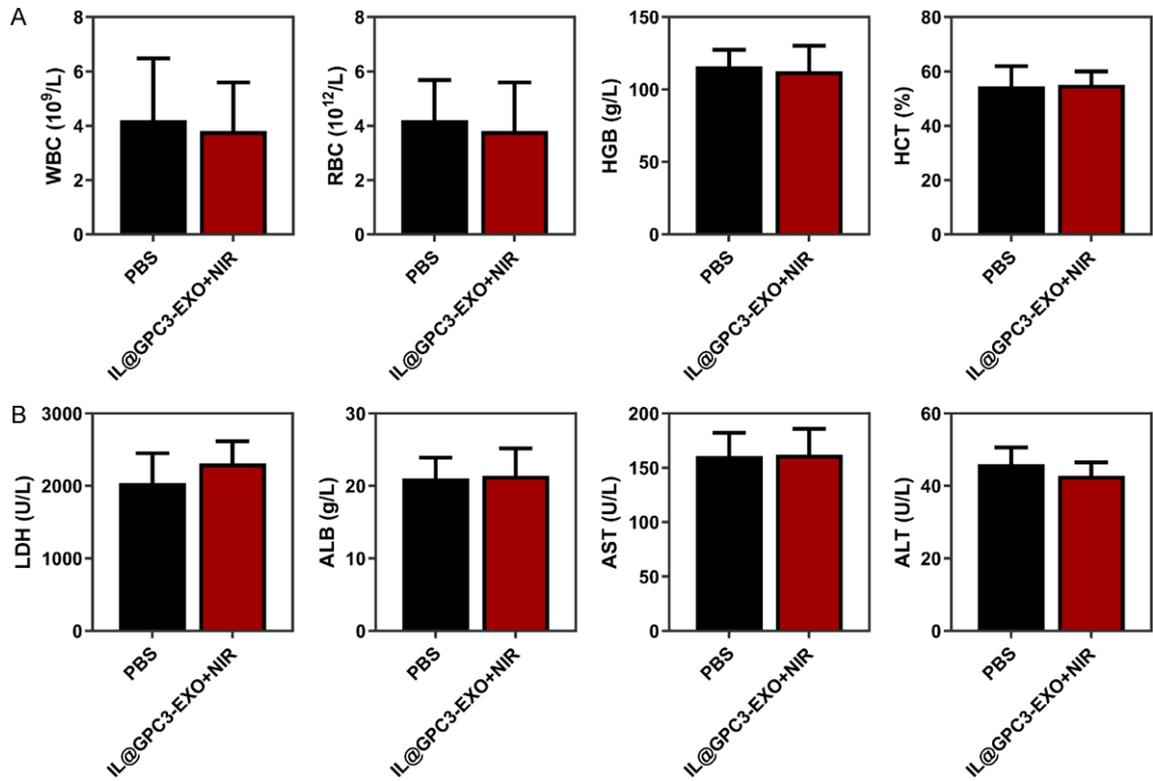

Figure S6. A, B. Parameter analysis for serum blood routine index and biochemistry tests.